

**QUANTIFYING THE EFFECTS OF LOWER SEA LEVEL ON  
TROPICAL PACIFIC CLIMATE DURING THE LAST GLACIAL  
MAXIMUM**

A Thesis  
Presented to  
The Academic Faculty

by

Eleanor Middlemas

In Partial Fulfillment  
of the Requirements for the Degree  
Bachelor of Science in the  
School of Mathematics

Georgia Institute of Technology

MAY 2013

**COPYRIGHT 2013 BY ELEANOR MIDDLEMAS**

**QUANTIFYING THE EFFECTS OF LOWER SEA LEVEL ON  
TROPICAL PACIFIC CLIMATE DURING THE LAST GLACIAL  
MAXIMUM**

Approved by:

Dr. Kim Cobb, Advisor  
School of Earth and Atmospheric Science  
*Georgia Institute of Technology*

Dr. Emanuele Dilozenzo  
School of Earth and Atmospheric Science  
*Georgia Institute of Technology*

Dr. Doron Lubinsky  
School of Mathematics  
*Georgia Institute of Technology*

Date Approved: May 2, 2013

## **ACKNOWLEDGEMENTS**

First and foremost, I wish to thank my research advisor and co-advisor, Dr. Kim Cobb and Dr. Emanuele DiLorenzo. They have put a tremendous number of hours into this project while teaching me that conducting research is challenging, tiring, but more importantly, fun and inspiring. I also wish to thank Dr. David Murphy and Dr. Jeannette Yen, both who introduced me to the world of academia. Working in both of these labs has paved a sturdy path for my plans for pursuing a doctorate as the next step in my life.

I would also like to acknowledge my family, who have supported and motivated me to pursue what I enjoy.

# TABLE OF CONTENTS

|  | Page |
|--|------|
| ACKNOWLEDGEMENTS                         | iv   |
| LIST OF FIGURES                          | vi   |
| LIST OF ABBREVIATIONS                    | vii  |
| SUMMARY                                  | viii |
| <u>CHAPTER</u>                           |      |
| 1 Motivation/Background                  | 1    |
| 2 Methods                                | 4    |
| Information about the Climate Model      | 4    |
| Climate Model Set-Up                     | 4    |
| 3 Results and Discussion                 | 7    |
| Mean State Changes                       | 7    |
| Response of El Nino-Southern Oscillation | 10   |
| 4 Conclusions                            | 13   |
| 5 Implications for Future Work           | 14   |
| REFERENCES                               | 16   |

## LIST OF FIGURES

|  | Page |
|--|------|
| Figure 3.1.1: Mean Precipitation   | 7    |
| Figure 3.1.2: Mean Vertical Velocity ( $\omega$ )                          | 8    |
| Figure 3.2.1: Precipitation Regressed on Nino34 Index                      | 10   |
| Figure 3.2.2: EOF1 of Mean Sea Level Pressure                              | 10   |
| Figure 3.2.3: Sea Level Pressure PC1 Regressed on Sea Surface Temperatures | 10   |

## LIST OF ABBREVIATIONS

|        |   |
|--------|---|
| GCM    | Global Climate Model                                      |
| AGCM   | Atmospheric Global Climate Model                          |
| AOGCM  | Atmosphere-Ocean Global Climate Model                     |
| SPEEDY | Simplified Parameterizations, primitive-Equation Dynamics |
| LGM    | Last Glacial Maximum                                      |
| ENSO   | El Nino-Southern Oscillation                              |
| MSLP   | Mean Sea Level Pressure                                   |
| MSLPa  | Mean Sea Level Pressure anomalies                         |
| SST    | Sea Surface Temperature                                   |
| SSTa   | Sea Surface Temperature anomalies                         |
| ITCZ   | Intertropical Convergence Zone                            |
| EOF    | Empirical Orthogonal Function                             |
| PC     | Principal Component                                       |
| PDO    | Pacific Decadal Oscillation                               |
| CESM   | Community Earth System Model                              |
| NOAA   | National Oceanic and Atmospheric Administration           |
| NCAR   | National Center for Atmospheric Research                  |



## SUMMARY

Global climate changes during the Last Glacial Maximum (LGM) have been ascribed to a combination of lower atmospheric CO<sub>2</sub>, increased albedo, large continental ice sheets, and altered ocean circulation. The effect of lowered sea level on LGM climate is typically considered negligible, despite the exposure of a continent-scale landmass, the Sunda Shelf, between Southeast Asia and Australia in the tropical Indo-Pacific.

Paleoclimate records document profound changes in tropical Indo-Pacific climate during the LGM, including weaker ENSO (Tudhope et al, 2001), changes in the sea-surface temperature gradient along the equatorial Pacific (Lea et al, 2000; Koutavas et al, 2002), and changes in western Pacific hydrology (Martinez et al 1997; Oppo et al, 2003). A recent investigation of coupled atmosphere-ocean general circulation model (AOGCMs) simulation of LGM climate suggests that the emergence of the Sunda Shelf alone may have reshaped tropical Indo-Pacific climate, contributing to a significant reduction in the strength of the Walker circulation (DiNezio et al, 2011). If true, this would have profound implications for the attribution of LGM paleoclimate signals of proxy data from the Indo-Pacific region. For example, regional drying inferred by a Sunda Shelf record during the LGM may be entirely ascribed to sea level change, and counter the regional hydrological response to cooler global temperatures and reduced pCO<sub>2</sub> during the LGM. The only modeling experiment that isolated the effects of lowered LGM sea level on climate documented significant atmospheric circulation changes spanning the entire tropical Pacific (Bush, et. al., 2003).

Here we present the results of lowered sea level simulations with the AGCM SPEEDY (Molteni, 2003) designed to gauge the sensitivity of tropical Pacific climate to

an LGM sea level drop of roughly 120m. Modifying the model's land/sea mask, we replaced ocean gridpoints in the East & South China Seas, the Gulf of Thailand, the Java Sea and the Arafura Sea with land gridpoints. As in the original mask, new land points were assigned values on a sliding scale of 0.1 to 1, depending on what percentage of the gridcell is ocean vs. land by our estimates. Both in the control run and the exposed land run, sea surface temperatures were prescribed along a tropical strip (-10-S to 10-N) to capture the atmospheric responses to realistic tropical SST variability associated with the El Nino-Southern Oscillation. Fifty ensembles of 60 years each were run for the control and for the Sunda Shelf experiment.

Our results show that the presence of the Sunda Shelf has the largest impacts in the vicinity of the new landmass, but impacts on large-scale atmospheric circulation variables are observed across the Pacific and Indian Ocean basins and extend into southern Asia. In the Sunda Shelf experiment, we observe significant changes in both near-surface winds and aloft wind fields, implying shifts in both the Walker and Hadley circulations. Precipitation decreases along the western portion of the Pacific Intertropical Convergence Zone, reflecting large-scale changes in wind fields, and accompany large-scale changes in sea-level pressure.

# **CHAPTER 1**

## **MOTIVATION/BACKGROUND**

Rising CO<sub>2</sub> levels, temperatures, and sea level all play a role in today's climate system. They remain a concern, since a changing climate could impact the everyday lives of humans. Therefore, we must understand how each climatic component impacts one another to be able to predict how weather may change in the future. Our focus is to investigate how the Earth will respond when sea level changes.

A specific time period of interest to paleoclimatologists is the Last Glacial Maximum, when the climate was very different from present: a significant portion of the Earth was covered by ice sheets. Because of the contrast to modern climate, the LGM is a useful time period to investigate the relationships between different climatic components. There are many proxy data that provide information about the climate during this period, such as lower atmospheric CO<sub>2</sub>, increased albedo, and altered ocean circulation, but they provide an incomplete picture of how climate dynamics differed during the LGM. Therefore, we must utilize a global climate model to understand the relationships between components, patterns of climate change, and what drives these changes.

The climate system's sensitivity to a given climate forcing can be gauged by investigating the effects of changes in that climate forcing. The effect of a 120m sea level fall is typically considered negligible during the LGM, despite the presence of an exposed continental-sized landmass in the Indo-Pacific, referred to as the "Sunda Shelf" (Bush et al., 2003). Sea level had huge impacts on the distribution of land and ocean, especially in the tropical Pacific, as shown by paleoclimate proxy records. These proxy

records indicate that during the LGM, El-Nino Southern Oscillation was weaker (Tudhope et. al., 2001), the sea-surface temperature gradient along the equatorial Pacific may have changed (Lea et al., 2000; Koutavas et al., 2002), and that the western Pacific may have been drier than today (Martinez et al., 1997; Oppo et al., 2003). The only modeling experiment that attempted to isolate the effects of the Sunda Shelf on LGM climate documented significant changes in the tropical Pacific atmospheric circulation (Bush et al., 2003). A recent survey of coupled ocean-atmosphere climate models found that the Sunda Shelf drove a weakening of Warm Pool convection that varied in strength among the different models (DiNezio et al., 2011).

We construct an experiment to isolate the effects of an exposed landmass in the Indo-Pacific region. We utilize an AGCM with an altered land/ocean distribution reflecting lowered sea level during the LGM quantifies the effects of the exposed Sunda Shelf on tropical Pacific climate, including El Nino-Southern Oscillation (ENSO) characteristics. The altered simulations will be compared against control simulations run with modern day sea level.

Global climate models (GCMs) are used in climate science to study the temporal and spatial evolution of climate under a variety of different conditions. These models utilize prescribed climate forcings and a set of dynamical equations to reproduce climate variability during a given time period. GCMs also can help characterize the relationship between the atmosphere and ocean, and their overall effect on global climate patterns. There are several different types of GCMs, including atmosphere-only models (AGCMs) that run with a “slab” ocean and prescribed ocean temperatures, and fully coupled ocean-atmosphere models (AOGCMs), where the ocean and the atmosphere are fully

interactive. Depending on the nature of the question, climate scientists employ either one or both of these models to probe the climate system's sensitivity to changes in climate forcings in the past, present, and future.

## CHAPTER 2

### METHODS

#### **2.1 *Information about the Climate Model***

Using remote computers on Dr. DiLorenzo's cluster, two experiments were executed using the atmospheric global climate model (AGCM) SPEEDY (Simplified Parameterizations, primitivE-Equation Dynamics (Molteni, 2008)). This model has a spatial resolution of 3.75 longitude by 3.7 latitude with 8 vertical levels in the atmosphere and a 50m slab ocean. In comparison to the numerous other climate models available, this model is considered extremely coarse for its time. The advantage to this coarseness is that it is not as costly, i.e., it does not require much computing time to return results. The disadvantage to the low-resolution of the model is that the effects of certain finer-scale processes may be lost. For example, the process of water eddies occurs on scales of meters to kilometers, which cannot be represented in this model. This model averages the effects of copious eddies inside one grid box, losing the potential consequences of any particular eddy. Because of this, we focused on first-order changes in the model.

#### **2.2 *Climate Model Set Up***

First, data was analyzed from a 60-year-long control simulation run with modern-day sea level. We assessed the strength of ENSO signals as a first metric, given ENSO's key role in shaping global climate patterns. We tried to apply as little forcing as possible to the model, in order to isolate the effects of the changes we incurred by adding land in the Indo-Pacific. The forcings that were applied in each experiment include daily sea

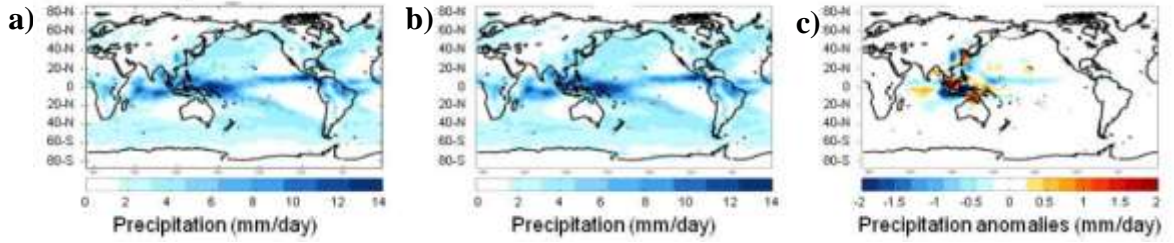
surface temperatures, which are prescribed from a modern National Oceanic and Atmospheric Administration (NOAA) reconstructed dataset (1950 – 2010) in a “tropical strip” (10-S to 10-N along the equator). This is used to capture the atmospheric responses to realistic tropical SST variability, with focus on the El Nino-Southern Oscillation. The two experiments had the same boundary condition configurations with the exception of a change of topography: a control run and a run with land added in the Indo-Pacific region (part of which was the Sunda Shelf). The control run has modern boundary conditions with present-day continental exposure. Adding land in the Indo-Pacific region simulates the additional exposure of land in this region during the Last Glacial Maximum. This land was generated by replacing ocean gridpoints with land gridpoints in the South and East China Seas, the Gulf of Thailand, the Java Sea, and the Arafura Sea. The land gridpoints were assigned on a sliding scale from 0.1 to 1.0 according to the percentage of land coverage within the gridcell; a value of 0.1 means that particular gridpoint has 10% land, while a value of 1.0 represents a gridpoint completely covered with land. Interpolation methods were used to determine what values to prescribe to monthly parameters such as land surface heat fluxes, skin temperature, and 3 layers of soil moisture, as well as constant parameters albedo, topography, and vegetation on the additional gridpoints. Ice cover and snow depth was not perturbed at all, since the area of concern does not lie within the boundaries of ice or snow cover.

Each run was for 60 years with 50 ensemble members to ensure statistical significance. We conducted the comparisons of climate variability with Matlab codes that we developed for this purpose. Variables compared in the altered versus control simulations include atmospheric responses such as mean annual precipitation, sea-surface

temperatures, sea level pressure, and in general, and characteristics of El Niño/La Niña events. Spatial averages were calculated by first, the averaging across the ~50 ensembles, and then averaging across time (from 1950-2010). A combination of statistical methods, including correlation and regression analysis, signal-to-noise ratios, empirical orthogonal function analysis, and singular value decomposition, were employed to investigate the climate signals of interest; the significance of any changes observed between the control and LGM simulations were assessed with a Monte Carlo approach.



### 3.1.1 Mean Precipitation



Plot (a) portrays present-day precipitation, (b) shows precipitation averages during the LGM (i.e., the presence of a Sunda Shelf), and (c) shows the changes incurred after adding a Sunda Shelf. Blue values signify a decrease in precipitation, and red values indicate an increase.

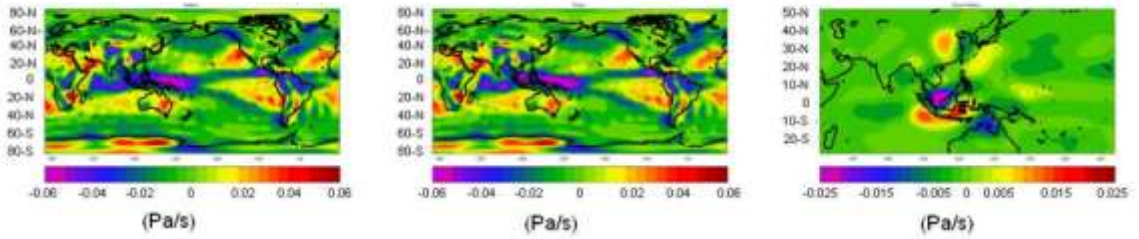
## RESULTS AND DISCUSSION

### 3.1 Mean State Changes

We explored a variety of model parameters related to changes in large-scale atmospheric circulation and precipitation caused by the emergence of the Sunda Shelf. Listed below is a record of the most robust changes observed.

Precipitation includes the response of multiple components of climate, so we report those changes as a first-order representation of our most robust results. The average precipitation, calculated by averaging all 50 ensemble member's precipitation over time, reveals that over the largest sections of the added gridpoints, precipitation increased, and immediately surrounding, precipitation decreased (Figure 3.1.1). This suggests that adding the land within the model offset the moisture budget by decreasing the amount of available moisture, so the model increased precipitation in that area. Since there must remain an equilibrium amount of water within the model, the model decreased the precipitation from surrounding areas. There is also a zonal pattern of decreased precipitation extending from the West Indian Ocean into the East Pacific Ocean,

### 3.1.2 Mean Vertical Velocity ( $\omega$ )



Mean Vertical Velocity has values on each of the 8 atmospheric levels. Left plot shows omega during present-day, the middle plot shows omega during the LGM, and the right plot portrays the changes in omega (LGM – present-day). Therefore, purple values indicate a decrease in vertical velocity, while red values indicate an increase.

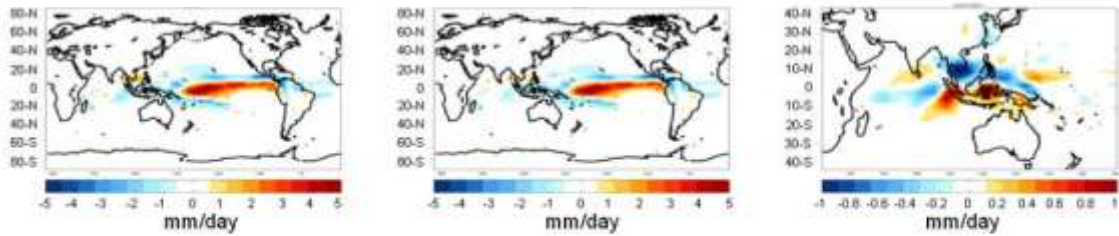
directly above the equator and somewhat equivalent to the location of the Intertropical Convergence Zone (ITCZ). This suggests a shift in the ITCZ but requires further investigation.

The changing pattern of precipitation confined to the modified land implies that changes in the Walker Cell should be considered. Therefore, we investigated changes in vertical velocity, which would reveal any shifts or robust changes in the Walker Cell. Calculated similarly to mean precipitation, the mean vertical velocity decreased more over the larger areas of exposed land, and increased immediately southward of the Sunda Shelf (Figure 3.1.2). This mirrors precipitation changes found previously, yet reveals no profound changes in the Walker Cell.

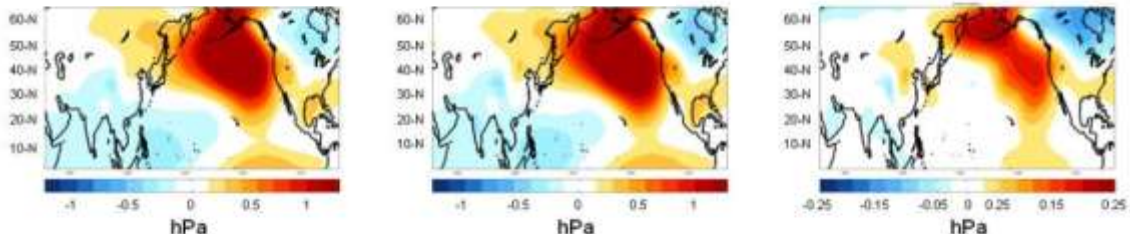
As we have prescribed SST's in the tropics, and most of our robust mean-state changes were found in the tropics, we cannot assume that these changes are completely realistic. This is because the responses from remaining interactive SST's across the globe may act differently than the prescribed SST's in the Tropics. Other less robust changes were observed in aloft wind fields and geopotential heights, but no patterns were

consistent, and may be explained by intrinsic variability. Further investigation, including a spatial statistical significance test, is necessary to validate this statement.

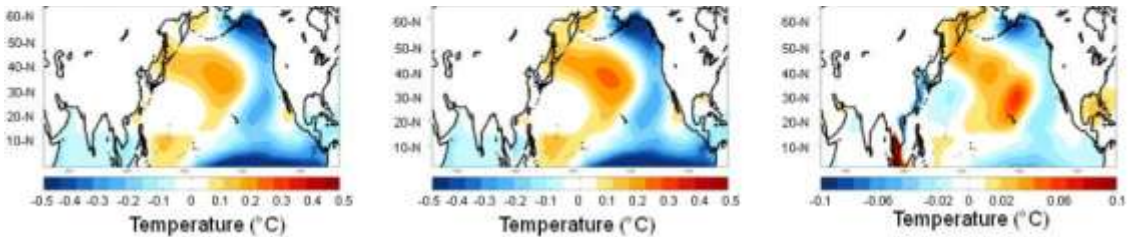
### 3.2.1 Precipitation Regressed on Nino34 index



### 3.2.2 First EOF of Mean Sea Level Pressure



### 3.2.3 PC1 of Sea Level Pressure Regressed on Sea-Surface Temperatures



All of the left plots portray present-day values, the middle plots portray LGM values, and the right plots show the differences between the two. Blue values in the difference plots indicate a decreased value, while red indicates an increased value.

## 3.2 Response of the El Nino-Southern Oscillation

We are particularly interested in responses in the extratropics that occur through teleconnections originating in the tropics, because we can pinpoint the cause of variability in areas all over the globe. As the tropics control much of the climate variability, prescribing SST's in the tropics would reveal any changes related to the El Nino-Southern Oscillation (ENSO), which occurs in the Tropical Pacific and on interannual timescales. As a first pass, a consideration of the spatial correlation and regression on the Nino34 index (an index representing El Nino variability) is required in order to determine if there is any existence of a relationship between a climate component

and ENSO. Correlation determines *the degree of similarity* of the variabilities of a component and El Nino, and the regression reveals how much the component varies *with respect to* Nino34. Typically, if there is an area of strong correlation between a component and Nino34, the spatial regression plot will reveal if that area of strong correlation actually represents a relationship between the two variables.

The precipitation correlation plot had strong signals over the newly exposed landmass, which led us to investigating the regression plot. This plot revealed that precipitation has decreased in response to ENSO in the northern area of the exposed landmass, and increased immediately southward (Figure 3.2.1). The fact that this reveals changes in variability with respect to El Nino, and it differs from the pattern of the mean state changes, implies that there are, in fact, changes occurring in our climate system on interannual timescales. It should be kept in mind that SST's are prescribed in the area where El Nino originates, suggesting that the atmosphere is responding to ENSO.

Next, empirical orthogonal function analysis (EOF's) was used to determine the spatial variation of a mean sea level pressure (MSLP), in order to understand variability in the movement of air in the atmosphere. Figure 3.2.2 shows the first mode of the EOF, which describes the most dominant form of spatial variability, of mean sea level pressure anomalies (MSLPa), in the northern hemisphere. There is a strong signal immediately south of Alaska, representing approximately 15% increased variability of the Aleutian Low, which we can conclude is likely in response to changes in ENSO, as we have prescribed SST's in the tropics. A statistical significance test is required to justify this statement, but a similar response was consistent in other analyses, such as the first mode EOF in of geopotential height at 500 mb in the northern hemisphere. Next, the principal

component (PC) was calculated, which represents the most dominant form of variability in the time domain. We regressed the PC of MSLPa on SSTs to reveal changes in this relationship. A pattern similar to the Pacific Decadal Oscillation (PDO) is seen in the Northern Pacific, indicated that this oscillation is increased in spatial variability (Figure 3.2.3). Again, it is evident that there are changes associated with the Aleutian Low variability. These results show that atmospheric anomalies are consistent with stronger basin-scale responses to tropical ENSO variability.

## **CHAPTER 4**

### **CONCLUSIONS**

Exposing the Sunda Shelf surrounding areas has significant impacts on Indo-Pacific mean climate state climate, with large responses located in the Sunda Shelf region itself. Significant atmospheric changes extend into the western Indian Ocean and into the Northern Pacific. Comparisons with proxies from these regions awaits a similar experiment performed with a fully-coupled climate model with the Sunda Shelf exposed, but it is clear that the Sunda Shelf likely altered precipitation in the vicinity of the landmass, as found in previous work, as well as atmospheric circulation in the North Pacific. It is critically important to distinguish the sea level response in Indo-Pacific proxies of LGM climate from the climate response associated with lower CO<sub>2</sub>/cooler global temperatures, in order to better constrain how this region may respond to rising temperatures in the coming decades.

## **CHAPTER 5**

### **IMPLICATIONS FOR FUTURE WORK**

We can obtain a more accurate representation of the presence of land in the Indo-Pacific during the LGM by prescribing cooler land-surface temperatures on the Sunda Shelf. This will provide a more realistic picture of the effects that were incurred from this exposed land. After adding this boundary condition, the next step of this experiment is to further develop our conclusions about mean state changes. This involves removing the forcings of SST's in the strip in tropical pacific, and allowing interactive SST's globally. As the tropical pacific is the control area for ENSO, prescribing SST's in that region allowed us to focus on changes in the climatic response to ENSO. To achieve a better understanding of annual mean state changes, rather than interannual, we will look at what happens when we allow the entire globe to interact with SSTs after altering the land/sea mask.

Considering the significant response of the atmospheric circulation patterns to the presence of the Sunda Shelf in SPEEDY, it is important to investigate how the response varies in a coupled ocean-atmosphere model such as the Community Earth System Model (CESM), provided by National Center for Atmospheric Research (NCAR). The suite of atmospheric signals presented here may either be damped for amplified by ocean-atmosphere coupling. The largest change in LGM land/ocean configuration, apart from the Sunda Shelf, is the closure of the Bering Strait. This may have effects on the ocean's thermohaline circulation, and/or impact North Pacific ocean-atmosphere climate variability. If so, then this would have consequences for the buildup or maintenance of



large continental ice sheets in North American and Eurasia. Future work will focus on simulating the climate effects of a closed Bering Strait.

## REFERENCES

- Bush, A.B.G, Fairbanks, R.G. “Exposing the Sunda shelf: Tropical responses to eustatic sea level change.” *Journal of Geophysical Research* 108 (2003): 1-10.
- DiNezio, P.M., Clement, A., Vecchi, G.A., et al. “The response of the Walker circulation to Last Glacial Maximum forcing: Implications for detection in proxies.” *Paleoceanography* 26 (2011): 1-26.
- Koutavas, A., Lynch-Stieglitz, J., Marchitto, T.M., et. al. “El Nino-like pattern in ice age tropical Pacific sea surface temperature.” *Science* 297 (2002): 226-230.
- Lea, D.W., Pak, D.K., Spero, H.J. “Climate impact of the late quaternary equatorial Pacific sea surface temperature variations.” *Science* 289 (2000): 1719-1724.
- Martinez, J.I., DeDeckker, P., Chivas, A.R. “New estimates for salinity changes in the Western Pacific Warm Pool during the Last Glacial Maximum: oxygen-isotope evidence.” *Marine Micropaleontology* 32 (1997): 311-340.
- Molteni, F. “Atmospheric simulations using a GCM with simplified physical parametrizations. I: model climatology and variability in multi-decadal experiments.” *Climate Dynamics* 20 (2003): 175-191.
- Oppo, D.W., Linsley, B.K., Rosenthal, Y., et. al. “Orbital and suborbital climate variability in the Sulu Sea, western tropical Pacific.” *Geochemistry Geophysics Geosystems* 4 (2003).
- Tudhope, A.W., Chilcott, C.P., McCulloch, M.T., et. al. “Variability in the El Nino-Southern oscillation through a glacial-interglacial cycle.” *Science* 291 (2001): 1511-1517.